Received: December 30, 2022. Revised: February 21, 2023.

INASS

International Journal of
Intelligent Engineering & Systems

http://www.inass.org/

Improved ABC Algorithm Based 3D Otsu for Breast Mass Segmentation in Mammogram Images

Ajay Mamindla[1]* **Ramadevi Y[2]**

[1] *Osmania University, India*
[2]*Chaitanya Bharati Institute of Technology, India*
* Corresponding author's Email: ajaymamindla@gmail.com

Abstract: One of the most prominent indicators for the detection of breast cancer is a breast mass. In this regard, effective mass segmentation for any type of mammography is crucial for improving breast cancer detection accuracy and lowering mortality. In order to pace up the process of mammogram segmentation for breast mass, an ABC3D (artificial bee colony based 3 dimensional) Otsu method is proposed in this paper. Firstly, convergence speed of bees in basic artificial bee colony (ABC) is improved by adopting the epsilon greedy method for scout bees. Secondly, proposed improved ABC method is paired with optimal 3D Otsu multilevel thresholding technique to get the better thresholding set for medical mammogram images. Epsilon greed based scout bee technique streamline the exploration-exploitation problem of standard ABC while searching for best threshold set in 3D space. The proposed ABC3D is tested on eight mammogram images collected from the authoritative and publicly available database mini MIAS (mammographic image analysis society). PSNR (peek signal to noise ration), SSIM (structural similarity index) and time cost are measured to record the effectiveness of ABC3D method. The results of experimentations indicate that the proposed ABC3D achieve superior segmentation results than the teaching learning ABC (TLABC), ABCDS (directed scout), gbest guided ABC (GABC), improved particle swarm optimization (IPSO) with 3D Otsu as objective functions.

Keywords: Mammogram segmentation, Artificial bee colony, 3D Otsu, Multilevel thresholding, Particle swarm optimization.

1. Introduction

Breast cancer illness has surpassed lung cancer as the most frequent cancer worldwide, according to the world health organization (WHO) in 2021 [1]. Breast cancer has the highest incidence rate of any malignant tumour in the world, making up around 10.4% of all malignancies [2]. In comparison to the 13% (1 in 8) diagnosed rate, around 1 in every 39 women (or 3%) will pass away from breast cancer throughout their lifetime [2]. However, the subtype and stage of breast cancer have a significant impact on the likelihood of survival and the mortality rate can be lowered to 15% from 40% with early detection [3], so developing tools for the early and precise detection of malignant tumour and diagnosis of breast cancer is essential. In past two decades, many more methods for image segmentation have been proposed. Due to its straightforward implementation, minimal processing requirements, and improved efficiency, the multi-threshold image segmentation (MTIS) method has become a popular methodology to research and employ [4].

Furthermore, The Otsu thresholding approach [5], a discrete counterpart of fisher's discriminant analysis, was devised by Nobuyuki Otsu in this context. The Otsu approach includes selecting an appropriate threshold for picture segmentation via a full-scale search that enlarge the between-class variance [5]. However, for noise images, standard Otsu method or its enhancements could not be able to achieve the accurate results for noise or week images. To overcome the problem, in [6] Jianzhuang. L et al. developed a 2-D histogram-based Otsu thresholding (2-D Otsu) method and in [7] Jing et al.

proposed 3-D histogram-based Otsu method (3-D Otsu) to selects the best threshold value. In 2-D Otsu, special correlation and gray scale values are combined to build the 2-D the histogram. Whereas in 3-D Otsu, neighbourhood's median is considered as the additional third parameter. Although the 2-D Otsu method has been shown to produce good results for noise and distorted images, the pixels probabilities in the background and foreground regions were ignored in the classes of second and third of 2D histograms that were close to their ideal threshold vector, resulting in inferior segmentation results. [8].

In 3-D Otsu method, to deal with the 2-D Otsu disadvantage, in addition to neighbourhood means and pixel grey scale information, a 3D histogram technique has been devised that takes the median of neighbourhood components into consideration as the third parameter. This method is supposed to produce better thresholding outcomes with a lower signal-to-noise ratio and deformed images than previous 1D and 2D methods [7]. However, the inclusion of a third parameter to 3-D Otsu raises the time complexity to O(L3) when compared to the time complexity of 2-D Otsu. To reduce the time complexity of 3-D Otsu method several other methods have been proposed. Nevertheless, these proposed enhancements unable to reduce the processing time. So, A quicker and more automated optimum threshold selection technique is required to optimize the searching operation.

In this context, A useful technique is to employ a nature inspired optimization algorithms (NIOA) techniques to optimize the searching process. For example, PSO [9], ABC [10] and TLBO (teaching learning based optimization) [11]. In [12] Zaho et al. proposed a modified ant colony optimization (RCACO) method with chaotic intensification and random spare approaches to raise the processing performance of MTIS. Zhang et al. [11] presented a model to better the Otsu and Kapur's entropy stability and improves the performance. Yanqiao et al. [12] proposed fast 2-D Otsu based on modified PSO algorithm to improve the operation speed of 2-D method and to restrict the PSO to not tends to local optimal threshold.

Karaboga et al. [10] presented a novel NIOA called the ABC in 2005, which has better ability to find the solutions to optimal solutions and in 2007 the standard ABC is inculcated for effective performance. The traditional ABC method still has shortcomings such as low optimality finding accuracy and sluggish convergence time, particularly when addressing high-dimensional complicated problems. The algorithm's optimality seeking stability and capability to hop away from local optimum ability still has a lot of space for improvement. As a result, researchers have created several enhanced variants of ABC and applied them to a variety of areas. Zhu and Kwong [15] presented the GABC method, which was inspired by the PSO algorithm, and in which the global optimal value gbest was incorporated as the guidance in the neighbourhood search equation to enhance the convergence speed and applied for the optimization of numerical functions. Chen et al. [17] proposed a new metaheuristic hybrid method by combing the TLBO and ABC features called TLABC and employed for parameter estimation. To find good solutions, TLABC utilizes hybridized three search phases: employed bee teaching-based phase, onlooker bee learning-based phase, and scout bee generalized oppositional phase [17].

Garside et al. [27] proposed improved version of ABC algorithm CDABC to minimize total earliness and tardiness flow shop scheduling problem. In [28] authors improved ABC to optimal path planning and the results show that the proposed HABC works better than the original ABC in terms of average path length and standard deviation, with a decrease up to 25%. In [29] authors modified ABC algorithms to solve the optimal power flow problem and it outperform the original ABC by reducing the fuel 11.34% fuel cost, 49.26% of power losses and 16.70% of emission. Ewees et al. [19] combined the ABC and sine-cosine algorithm (ABCSCA) to improve MTIS effectiveness and used the suggested approach to segment images using Otsu and Kapur's entropy. Saleh et al [18] proposed ABCDS (directed scout) improved the performance of ABC and its more recent variations by altering the scout phase. This change improves its exploitation capability by enlarging the regions of the search space that are likely to include viable solutions. Hang Su et al. [13], proposed an improved ABC (CCABC) to improve the effectiveness of the MTIS method and showed effective performance in image segmentation of lung tissue.

However, recent ABC upgrades produced good results when compared to other NIOA techniques paired with one- and two-dimensional Otsu; there is room for improvement in solving the slow convergence problem, as well as utilizing the latest version 3-D Otsu to segment mammograms. The no-free-lunch (NFL) theorem states that not all optimization strategies can be applied to the same issue [14]. Although ABC has been applied to a different kind of optimization problems successfully, it still come across with delayed convergence and low quality of best solutions during the process of optimization [13]. In the ABC3D method, the traditional ABC method is first upgraded to deal with slow convergence of hive bees and linked with the 3-D Otsu function as the objective function to increase segmentation accuracy in medical images like mammograms. This study's main motivation is to suggest and test different possible solutions to multilevel thresholding problems using mammography segmentation.

This research main contributions could well be summarised as follows:

- This research proposes improved Scout bee-based ABC method.
- Proposed method is employed to Mammogram MTIS based on the 3-D histogram.
- The mammogram segmentation results are compared and tested with other state-of-art methods.

The remaining part of this work is organized as follows. In section 2, 1D, 2D Otsu function and Original ABC algorithms are discussed. In section 3, 3-D Otsu basic formulation and the proposed method in brief. Experimental outcomes and comparison analysis are illustrated in section 4, and in section 5, conclusions and future scope are presented.

2. Previous works and motivation

Recent contributions focus on applying recently discovered optimization methods to multilevel thresholding-related tasks [16, 18]. New thresholding approaches with higher accuracy and more information richness in segmented images are being presented nowadays [19, 13]. Conspicuously, using NIOA-based image segmentation algorithms, the mass tissue in the breast could be accurately and efficiently segmented. The need for improved segmented mammograms is challenging and significant. This is the driving force of our paper. ABC was chosen from among the NIOA-based algorithms because it has advantages such as resilience, flexibility, exploring local solutions, and broad application.

A. 1-Dimentional Otsu thresholding

Suppose L indicates the image gray level, fk denotes kth Level pixel points count, then the pixel total points are calculated as Eq. (1).

$$M = \sum_{k=1}^{L} f_k \tag{1}$$

After calculating the total pixel points then probability density distribution of ID-Histogram is represented as Eq. (2).

$$\boldsymbol{p_k = \frac{f_k}{M}, \quad \sum_{k=1}^{L} p_k = 1 \quad\quad p_k \geq 0} \tag{2}$$

Assume the threshold 'h' separates the picture into two groups, such as background group G0 and foreground group G1.

$$G_0 = \{1, 2, ..., h\};\ G_1 = \{h+1, h+2, ..., L\}$$

Assume $\boldsymbol{\delta_V^2}$ denotes between-class divergence, then the optimal threshold h' fulfils the following Eq. (3).

$$\boldsymbol{\delta_V^2(h') = \max_{1 \leq T\alpha L}\{\delta_V^2(h)\}} \tag{3}$$

B. 2-Dimentional Otsu thresholding

The troughs and peaks and of the histogram were separated by employing threshold values in 1-D Otsu, and the image segmentation outcome result is larger than the pixels threshold values given to the background colour, while the remaining are given to target, and vice versa. Even so, in exercise, noise intervention and other related factors cause the image histogram distribution to be not always noticeable troughs and peaks, so using 1-D Ostu thresholding cannot always produce acceptable results for image segmentation, and major segmentation mistakes can take place [20]. Therefore, the researchers offer a 2-D thresholding [6] technique based on a 2-d grey histogram. Consider how a threshold vector (h, t) might separate pixels in an image into two classes: background class G0 and foreground class G1. In 2-D Otsu's method, A 2-D histogram design is used, which is generated by taking the neighbouring components mean and intensity information into account. The incidence probabilities of these two groups are calculated as Eqs. (4) and (5):

$$\boldsymbol{\omega_0 = \sum_{k=0}^{h} \sum_{j=0}^{t} p_{kj}} \tag{4}$$

$$\boldsymbol{\omega_1 = \sum_{k=h+1}^{L-1} \sum_{j=t+1}^{L-1} p_{kj}} \tag{5}$$

Classes G0 and G1 mean is formulated as Eqs. (6) and (7):

$$\boldsymbol{\mu_0 = \left(\sum_{k=0}^{h} \sum_{j=0}^{t} \frac{k \cdot p_{kj}}{\omega_0}, \sum_{k=0}^{h} \sum_{j=0}^{t} \frac{j \cdot p_{kj}}{\omega_0}\right)^T} \tag{6}$$

Received: December 30, 2022. Revised: February 21, 2023.

$$\mu_1 = \left(\sum_{k=h+1}^{L-1}\sum_{j=t+1}^{L-1}\frac{k\cdot p_{kj}}{\omega_1}, \sum_{k=h+1}^{L-1}\sum_{j=h+1}^{L-1}\frac{j\cdot p_{kj}}{\omega_1}\right)^T \quad (7)$$

2-D histogram total mean is Eq. (8)

$$\mu_T = \left(\sum_{k=0}^{L-1}\sum_{j=0}^{L-1} k\cdot p_{kj}, \sum_{k=0}^{L-1}\sum_{j=0}^{L-1} j\cdot p_{kj}\right)^T \quad (8)$$

Formula for between class variance Eq. (9):

$$\sigma_V^2(h,t) = w_0[(\mu_0-\mu_T)(\mu_0-\mu_T)^T] + w_1[(\mu_1-\mu_T)(\mu_1-\mu_T)^T] \quad (9)$$

Optimal Threshold array is Eq. (10)

$$(h',t') = \underset{0\le h,t\le L-1}{arg\,max}\{\sigma_V^2(h,t)\} \quad (10)$$

Input Image, I, is segmented for various threshold levels N using Threshold set Eq. (11) as:

$$\left\{\frac{h_1'+t_1'}{2}, \dots, \frac{h_{N-1}'+t_{N-1}'}{2}\right\} \quad (11)$$

C. 3-Dimentional Otsu thresholding

In the 3-D histogram representation [25], Assume the size of given image is MxN. (u,v) denotes the coordinate point of element, f(u,v) represents the gray values of the coordinate point, g(u,v) (Eq. (12)) is d x d gray level neighbourhood average and h(u,v) (Eq. (13)) is d x d lever gray level neighbouring variance, then

$$g(u,v) = \frac{1}{d*d}\sum_{m=-\frac{d-1}{2}}^{\frac{d-1}{2}}\sum_{n=-\frac{d-1}{2}}^{\frac{d-1}{2}} f(u+m, v+n) \quad (12)$$

$$h(u,v) = (f(u,v) - g(u,v))^2 \quad (13)$$

The cube area of the 3D histogram with a size of L x L x L is where it is constrained. By expressing an input image using the 3D vector [f(u, v),g(u, v),h(u, v)] and having rjkl represent the overall frequency of pair (j, k, l) if j= f(u, v), k= g(u, v), l=h(u, v). Fig. 1 shows the 3-D histogram and its rectangular volumes.

3-D histogram point is formulated as Eq. (14) with min and max values of pixel values is 0 and n respectively.

$$P_{jkl} = \frac{C_{jkl}}{M\times N} \quad (14)$$

Where j,k =0 to n.

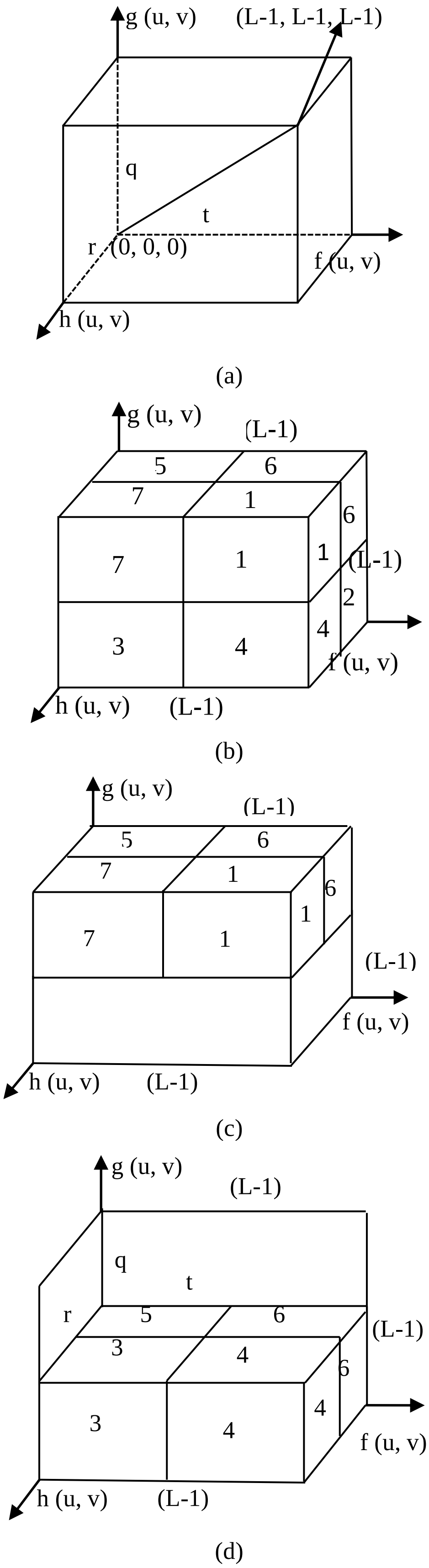

Figure. 1 3D Histograms: (a) 3-D histogram in cube LxLxL (b), (c), and (d) are eight elements of 3-D histograms

 DOI: 10.22266/ijies2023.0430.50

Now, assume that the G0 and G1 are the two portioned classes of pixels by a pair of thresholds (r, q, t). Go and G1 probabilities are given as Eqs. (15) and (16):

$$\boldsymbol{\omega_0} = \sum_{(j,k,l)\in G_0} \boldsymbol{P_{jkl}} = \sum_{j=0}^{r} \sum_{k=0}^{q} \sum_{l=0}^{t} \boldsymbol{P_{jkl}} \quad (15)$$

$$\boldsymbol{\omega_1} = \sum_{(j,k,l)\in G_1} \boldsymbol{P_{jkl}} = \sum_{j=r+1}^{L-1} \sum_{k=q+1}^{L-1} \sum_{l=t+1}^{L-1} \boldsymbol{P_{jkl}} \quad (16)$$

Corresponding Mean values of G_0 and G_1 are Eqs. (17) and (18)

$$\begin{aligned}\boldsymbol{\mu_0} &= \left(\boldsymbol{\mu_{0j}}, \boldsymbol{\mu_{0k}}, \boldsymbol{\mu_{0l}}\right)^{\boldsymbol{T}} \\ &= \Bigg(\frac{1}{\boldsymbol{\omega_0}}\sum_{j=0}^{r} \sum_{k=0}^{q} \sum_{l=0}^{t} \boldsymbol{jP_{jkj}}, \\ &\quad \frac{1}{\boldsymbol{\omega_0}}\sum_{j=0}^{r} \sum_{k=0}^{q} \sum_{l=0}^{t} \boldsymbol{jP_{jkl}} \\ &\quad \frac{1}{\boldsymbol{\omega_0}}\sum_{j=0}^{r} \sum_{k=0}^{q} \sum_{l=0}^{t} \boldsymbol{kP_{jkl}}\Bigg)^{\boldsymbol{T}}\end{aligned} \quad (17)$$

$$\begin{aligned}\mu_1 &= \left(\mu_{1j}, \mu_{1k}, \mu_{1l}\right)^{T} \\ &= \left(\begin{array}{l}\frac{1}{\omega_1}\sum_{j=r+1}^{L-1} \sum_{k=q+1}^{L-1} \sum_{l=t+1}^{L-1} jP_{jkl}, \\ \frac{1}{\omega_1}\sum_{j=r+1}^{L-1} \sum_{k=q+1}^{L-1} \sum_{l=t+1}^{L-1} kP_{jkl}, \\ \frac{1}{\boldsymbol{\omega_1}}\sum_{j=r+1}^{L-1} \sum_{k=q+1}^{L-1} \sum_{l=t+1}^{L-1} \boldsymbol{lP_{jkl}}\end{array}\right)^{\boldsymbol{T}}\end{aligned} \quad (18)$$

The vector of 3-D Histogram total mean is Eq. (19)

$$\boldsymbol{\mu_T} = \left(\boldsymbol{\mu_{Tj}}, \boldsymbol{\mu_{Tk}}, \boldsymbol{\mu_{Tl}}\right)^{\boldsymbol{T}} = \left(\begin{array}{c}\sum_{j=0}^{L-1L-1} \sum_{k=0}^{L-1} \sum_{l=0}^{L-1} \boldsymbol{jP_{jkl}}, \sum_{j=0}^{L-1L-1} \sum_{k=0}^{L-1} \sum_{l=0}^{L-1} \boldsymbol{kP_{jkl}}, \\ \sum_{j=0}^{L-1} \sum_{k=0}^{L-1} \sum_{l=0}^{L-1} \boldsymbol{lP_{jkl}}\end{array}\right)^{\boldsymbol{T}} \quad (19)$$

Background class and target class discrete matrix is measured as Eq. (20):

$$\boldsymbol{S_V} = \boldsymbol{\omega_0}[(\boldsymbol{\mu_0} - \boldsymbol{\mu_T})(\boldsymbol{\mu_0} - \boldsymbol{\mu_T})^{\boldsymbol{T}}] + \boldsymbol{\omega_1}[(\boldsymbol{\mu_1} - \boldsymbol{\mu_T})(\boldsymbol{\mu_0} - \boldsymbol{\mu_T})^{\boldsymbol{T}}] \quad (20)$$

SV trajectory is used as dispersion criterion for 3-D Otsu and measured as Eq. (21)

$$\begin{aligned}\mathbf{t_r S_V} &= \boldsymbol{\omega_0}\left[\left(\boldsymbol{\mu}_{\mathbf{0j}} - \boldsymbol{\mu}_{\mathbf{Tj}}\right)^{\mathbf{2}} + (\boldsymbol{\mu}_{\mathbf{0k}} - \boldsymbol{\mu}_{\mathbf{Tk}})^{\mathbf{2}} + (\boldsymbol{\mu}_{\mathbf{0l}} - \boldsymbol{\mu}_{\mathbf{Tl}})^{\mathbf{2}}\right] \\ &+\boldsymbol{\omega_1}\left[\left(\boldsymbol{\mu}_{\mathbf{1j}} - \boldsymbol{\mu}_{\mathbf{Tj}}\right)^{\mathbf{2}} + (\boldsymbol{\mu}_{\mathbf{1k}} - \boldsymbol{\mu}_{\mathbf{Tk}})^{\mathbf{2}} + (\boldsymbol{\mu}_{\mathbf{1l}} - \boldsymbol{\mu}_{\mathbf{Tl}})^{\mathbf{2}}\right] \\ &= \frac{[\mu_j - \boldsymbol{\omega_0}\mu_{Tj}]^2 + [\mu_k - \boldsymbol{\omega_0}\mu_{Tk}]^2 + [\mu_l - \boldsymbol{\omega_0}\mu_{Tl}]^2}{\boldsymbol{\omega_0}(\mathbf{1} - \boldsymbol{\omega_0})}\end{aligned} \quad (21)$$

Select the vector (T, Q, R) of optimal threshold by maximizing Eq. (22):

$$\boldsymbol{t_r S_V}(\boldsymbol{R}, \boldsymbol{Q}, \boldsymbol{T}) = \underset{\boldsymbol{0<r,q,t<n}}{\boldsymbol{max}} \{\boldsymbol{t_r S_V}(\boldsymbol{r}, \boldsymbol{q}, \boldsymbol{t})\} \quad (22)$$

D. Artificial bee colony

ABC is swarm intelligence (SI) based meta-heuristic algorithms developed by mimicking the foraging behavior of various bees in the Hive [10]. SI based methods are inspired by the distributive problem-solving abilities as a swarm. The two primary functions of any metaheuristic-based algorithm are exploitation and exploration. The primary characteristics of any swarm-based algorithm, such as ABC, are division of work and self-organization. unemployed foragers, employed foragers and Food sources are the three elements of bee colony. Depending on their extraction degree, closeness, and food content, food sources might be characterized by a "profitability" feature. Unemployed foragers are divided into two groups: scout bees (SB) and onlooker bees (OB). Onlooker bees search for good source of food by considering the waggle movements of an employee bee (EB), and SB search for another food sources in the neighbouring area if food source failure limit is exceeded [21]. The initialization phase is the first step in every meta-heuristic method.

To produce a random population of food sources (SN), apply Eq. (23).

$$\boldsymbol{x_k^i} = \boldsymbol{x_{min}^i} + \emptyset\left(\boldsymbol{x_{max}^i} - \boldsymbol{x_{min}^i}\right) \quad (23)$$

Where ‘i’ is randomly selected food source, min and max denotes the lower and upper bound of the ‘i-th’ solution. ∅ any value between (-1,1) chosen at random.

In the EB phase, present solution is changed with randomly chosen partner solution using the Eq. (24).

$$\boldsymbol{X_{new}^i} = \boldsymbol{X^i} + \emptyset\left(\boldsymbol{X^i} - \boldsymbol{X_P^i}\right) \quad (24)$$

Where ‘i’ is randomly chosen present solution, P is randomly chosen partner solution and ∅ any value between (-1,1) chosen at random. Based on the fitness value of a new solution ‘k’ calculated by Eq. (25), the present solution is updated and substituted by employed bees.

$$\boldsymbol{Fit}(\boldsymbol{k}) = \begin{cases} \mathbf{1/1} + |\boldsymbol{f}(\boldsymbol{k})| & \mathit{if}\, \boldsymbol{f}(\boldsymbol{k}) \geq \mathbf{0} \\ \mathbf{1} + |\boldsymbol{f}(\boldsymbol{k})| & \mathit{if}\, \boldsymbol{f}(\boldsymbol{k}) < \mathbf{0}) \end{cases} \quad (25)$$

In OB phase, every OB will travel to a source of food based on the quality information computed from the employee bees' food resources. Eq. (26) computes the probability of the food source quality. The greater the fitness value, the higher the probability of selection.

$$\boldsymbol{Prob_k} = \mathbf{0.9} \times \frac{\boldsymbol{Fit_k}}{\sum_{\boldsymbol{k=1}}^{\boldsymbol{n}} \boldsymbol{Fitk}} \quad (26)$$

In SB Phase, it is assumed that a food source has been depleted if it is not updated after a certain number of iterations. As a result, The EB then becomes a SB, and Eq. (24) generates a new food source randomly in the search region.

E. Epsilon-greedy method (EG)

Epsilon-greedy is an optimal strategy for balancing exploitation and exploration with ϵ -parameter by randomly selecting between those. The original EG policy is based on uniform distribution while choosing a candidate in 1- ϵ case [23].

$$P= \begin{cases} \boldsymbol{Best\_Candidate} & \mathit{if\ prob} \leq \boldsymbol{\epsilon} \\ \boldsymbol{new}\mathit{\_Random\_Candidate} & \mathit{prob} > \boldsymbol{\epsilon} \end{cases} \quad (27)$$

In case of NIOA algorithms, the ϵ -greedy strategy selects a random selection with a probability of 1- ϵ (exploration) and the current best candidate from a pool of candidates with a probability of ϵ (exploitation) from Eq. (27). For Example, PSO algorithm is improved by adopting EG policy in case of exploitation-exploration (EE) dilemma [24].

3. Proposed methodology

A. Scout bee based improved ABC

In standard ABC algorithm and it's all proposed multiple versions, exploration is increased in the SB phase. EB turns to SB to abandon the present solution if it exceeds the limit specified. In the SB phase, SB replaces the abandoned food origin with the oppositional food source or randomly selection food source. As a result, most of the ABC versions exploration is chosen over exploitation. In ABCDS (directed scout bee) variation, most of the time exploitation is chosen instead exploration, which leads to decreasing of exploration for new solutions. Consequently, SB in a crossroads of exploitation-exploration dilemma, to choose a new solution (exploration) or continue with the current best solution of this area (exploitation). Therefore, in this research, scout bee adopts the ϵ -greedy strategy to solve the EE dilemma. Firstly, when a food source exceeds its limit then the EB turns to SB and using the Eq. (28) it selects either the exploitation of current best solution in the area using local search or selects the new food source at randomly.

$$P= \begin{cases} \boldsymbol{X\_best\_sol} & \mathit{if\ prob} \leq \boldsymbol{\epsilon} \\ \mathit{X\_New\_sol} & \mathit{prob} > \boldsymbol{\epsilon} \end{cases} \quad (28)$$

Where X_best_sol is the best food source memorized till then. And X_new_sol is the new food source selected randomly using Eq. (24). Therefore, in the case X_best_sol SB is restricted to search in the most promising area achieved so far in the solution space, in X_New_sol case, SB selects the probably the best new solution comparatively. Improved ABC pseudo code is given as follows:

Pseudo-code for improved ABC:

1. Initialize the solution (SN) using Eq. (23)
2. Calculate each solution fitness value using (25)
3. Repeat //EB Phase
4. For k= 1 to SN do
5. Produce new solution (X_{new}) with Eq. (24)
6. End For //End of EB; Start of OB Phase
7. Find Food source probability with Eq. (26)
8. For k=1 to SN do
9. OB chooses the Food source based on selection probability
10. Generates X_{new} solution using Eq. (24)
11. End For //END OB; Start of SB Phase
12. Identity the maximum failure solution
13. If Failure >=Limit, then
14. Find $\boldsymbol{\epsilon}$ -greedy Probability with Eq. (28)
15. If prob <= $\boldsymbol{\epsilon}$ then select best solution memorized so far
16. Else Find random X_{new} using Eq. (24)
17. End if
18. End if // End of SB Phase
19. Remember the Best Solution (X_{best_sol})

B. Proposed ABC3D methodology

The process of determining the ideal threshold is referred to as an optimization method with the Eq. (9) objective function. Finding the collection of triple vectors (r, t, q) that maximizes Eq. (22), Evaluation of fitness function, is the primary goal of this optimization. traditional 3-D Otsu identifies the vector of ideal thresholds that optimizes the between-class variance after doing an exhaustive search that checks each conceivable threshold.

Eq. (28) reduces the exhaustive search time by finding solution to the exploitation-exploration, which is the secondary goal of this method. the ABC population is first created at random and restricted by lower and upper limits by Eq. (23). Each SV indicates a potential response to a set of thresholds (ri, ti, qi), where ri represents intensity, ti indicates mean and qi stands for median thresholds in the considered neighbourhood pixels, respectively. The triplet (ri, ti, qi) elements are sealed off to nearest original integers, which are utilized for thresholding since the image pixel value is defiantly an integer value.

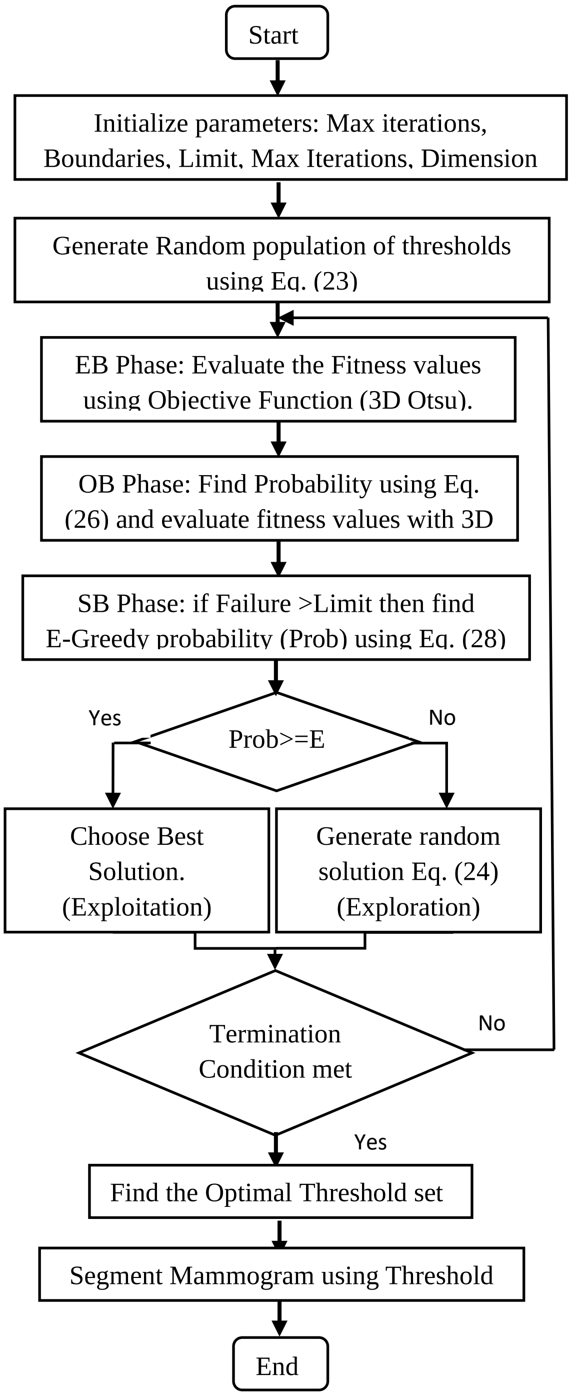

Figure. 2 Proposed improved ABC (ABC3D) process

In improved ABC, fitness is determined using Eq. (22) at each iteration point, and the best solution currently available Xi is returned. This is then compared to previously memorized best solution X_best_sol. The ultimate best possible solution, X_best_sol, is returned when the halting requirement is met in accordance with Improved ABC. The threshold vector is defined as the point that corresponds to X_best_sol. Any triplet (ri, ti, qi) element that exceeds L during optimization will be replaced with a random number in the range (0, L-1). The provided image is segmented appropriately using the threshold vector that the Improved ABC algorithm returned. Pseudo code gives a description of the Improved ABC related phases and the entire flow diagram for the suggested Improved ABC-based 3-D Otsu is shown in Fig. 2. The notion of newly Improved ABC is being applied with 3-D Otsu for the first time in mammogram image segmentation, demonstrating the potential of image segmentation to accomplish a wide class of goal in the field of medical imaging.

4. Experimental results and analysis

A. Experimental settings

The developed algorithm's performance is illustrated using mammograms dataset called MIAS [26], which is publicly available on the (http://peipa.essex.ac.uk/info/mias.html) website. Fig. 5 first row shows the selection of eight MIAS mammograms for this investigation. The proposed algorithm is applied on the selected images with the thresholds (K-1) starting from 1 to 5. Single level thresholding is indicated with (K-1) =1, and MTIS is applied with (K-1) =2, 3 and 5. In IABC, lower bound and upper bound are set to 0 and 256 respectively. Solution population (SN) is depending on mammogram histogram and number of iterations and limit are considered as 10 and 20 respectively for all investigations.

B. Performance measurements

In this study, performance measuring parameters like PSNR (peak signal noise ratio), SSIM (structural similarity index) [22] and CPU time are used to present the comparative results of proposed method with the other state-of-art methods like TLABC, GABC, ABCDS and PSO. Among all, PSNR is most widely used parameter to indicates the final mammogram partition's region homogeneity. Good mammogram segmentation is depending on the higher PSNR values. Tables 1-3 show a quantitative evaluation of the thresholder images calculated by ABC3D and the other four

Received: December 30, 2022. Revised: February 21, 2023.

Table 1. SSIM value comparisons

	TLABC **[17]**	ABCDS **[18]**	GABC **[15]**	IPSO **[13]**	**ABC3D**
2-Thresholds					
Img1	0.824	0.828	0.827	0.83	0.831
Img2	0.822	0.829	0.834	0.83	0.824
Img3	0.779	0.873	0.783	0.788	0.885
Img4	0.779	0.784	0.782	0.796	0.881
Img5	0.818	0.812	0.823	0.742	0.813
Img6	0.818	0.794	0.824	0.82	0.818
Img7	0.792	0.801	0.797	0.812	0.797
Img8	0.869	0.765	0.777	0.877	0.771
3-Thresholds					
Img1	0.823	0.86	0.824	0.833	0.838
Img2	0.817	0.829	0.832	0.833	0.835
Img3	0.782	0.81	0.774	0.881	0.881
Img4	0.793	0.793	0.834	0.808	0.789
Img5	0.822	0.819	0.839	0.814	0.817
Img6	0.815	0.816	0.818	0.812	0.868
Img7	0.815	0.794	0.888	0.796	0.793
Img8	0.871	0.773	0.795	0.871	0.877
5-Thresholds					
Img1	0.863	0.828	0.824	0.832	0.823
Img2	0.837	0.831	0.829	0.829	0.825
Img3	0.772	0.803	0.881	0.887	0.889
Img4	0.811	0.778	0.783	0.811	0.884
Img5	0.827	0.82	0.854	0.823	0.819
Img6	0.821	0.823	0.817	0.819	0.816
Img7	0.804	0.799	0.785	0.798	0.885
Img8	0.879	0.808	0.869	0.829	0.875
AVG	**0.82**	**0.81**	**0.82**	**0.82**	**0.84**

Table 2. PSNR Value comparison

	TLABC **[17]**	ABCDS **[18]**	GABC **[15]**	IPSO **[13]**	**ABC3D**
2-Thresholds					
Img1	32.43	32.41	32.43	32.44	32.42
Img2	31.43	31.37	31.36	31.42	31.42
Img3	30.25	30.22	30.26	30.24	30.2
Img4	29.18	29.1	29.16	29.23	29.18
Img5	32.91	32.77	32.78	32.76	32.82
Img6	31.83	31.82	31.77	31.81	31.95
Img7	31.18	31.18	31.19	31.23	31.23
Img8	29.68	29.68	29.66	29.65	29.69
3-Thresholds					
Img1	32.41	32.43	32.5	32.41	32.44
Img2	31.27	31.43	31.42	31.4	31.44
Img3	30.28	30.26	30.29	30.23	30.21
Img4	29.14	29.26	29.18	29.2	29.48
Img5	32.75	32.78	32.81	32.86	32.84
Img6	31.86	31.81	31.82	31.86	31.8
Img7	31.2	31.25	31.27	31.25	31.19
Img8	29.62	29.64	29.66	29.66	29.73
5-Thresholds					
Img1	32.4	32.44	32.4	32.49	32.4
Img2	31.4	31.43	31.39	31.35	31.46
Img3	30.22	30.27	30.24	30.29	30.29
Img4	29.17	29.2	29.12	29.11	29.26
Img5	32.79	32.77	32.77	32.74	32.77
Img6	31.8	31.86	31.99	31.8	31.87
Img7	31.14	31.2	31.11	31.25	31.15
Img8	29.66	29.83	29.69	29.67	29.89
AVG	**31.07**	**31.13**	**31.09**	**31.09**	**31.14**

segmentation algorithms (TLABC, GABC, ABCDS and PSO with 3D Otsu as objective function). Even though they use the same fitness function, the threshold values achieved by different approaches are distinct. This is determined by the algorithm's search procedure. SSIM value comparison of all 5 selected methods are given in Table 1. The proposed approach based on ABC3D clearly outperforms other methods in the majority of the eight examined mammograms, Fig. 3 shows the graphical representation of the same with 3 thresholds.

Out of eight mammograms, proposed method with three thresholds achieves better results in 5 images. The PSNR values of ABC3D and other state of art methods are given in Table 2 and Fig. 4. According to Table 2, the 3-D Otsu technique based on the improve ABC (ABC3D) algorithm outperforms the other algorithms when comparing PSNR values ABC3D with other comparative methods in 6 out of 8 images. Moreover, in terms of average of PSNR and SSIM values of Tables 1 and 2, ABC3D have higher values than any comparative method. However, ABC3D still gave lower SSIM and PSNR values for few selected mammograms because of local minima problem. In addition, it is observed that SSIM results are improved when the number of thresholds increased and PSNR value is improved in five thresholds.

From Table 3, It may be inferred that reducing the threshold count will speed up the process. The ABC3D approach has the least amount of time to execute compared to other optimization-based methods. When can be seen from the Table 3, the execution time dramatically decreases as the number of thresholds is raised in comparison to other optimization-based approaches. This is as a result of the finding solution to the slow convergence in exploration-exploitation problem with epsilon greedy policy. The ABC3D approach outperforms the previous optimization techniques in terms of overall performance during execution. However, 3D Otsu takes more CPU time when compared to 1-D Otsu.

Fig. 5 illustrate the visual aspect of the proposed and comparative methods used in this work. First row indicated the eight images chosen randomly from the MIAS dataset and converted to gray level.

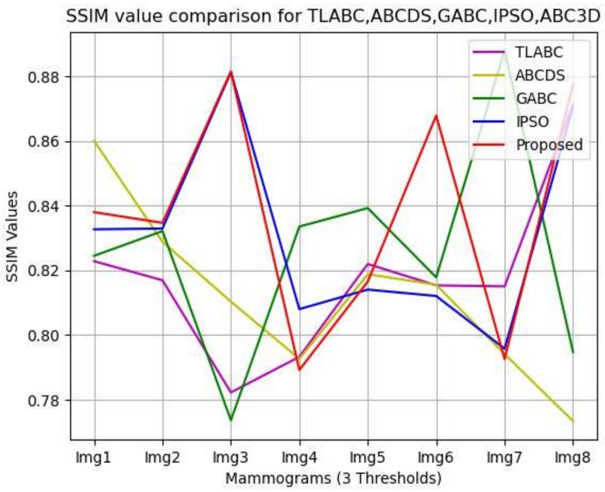

Figure. 3 SSIM values comparison

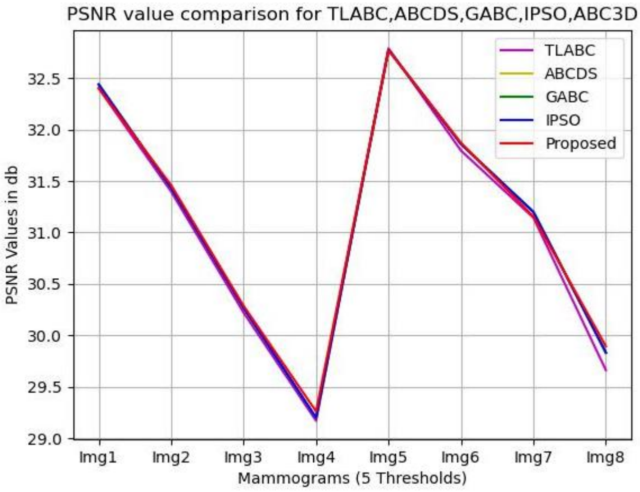

Figure. 4 PSNR value comparison

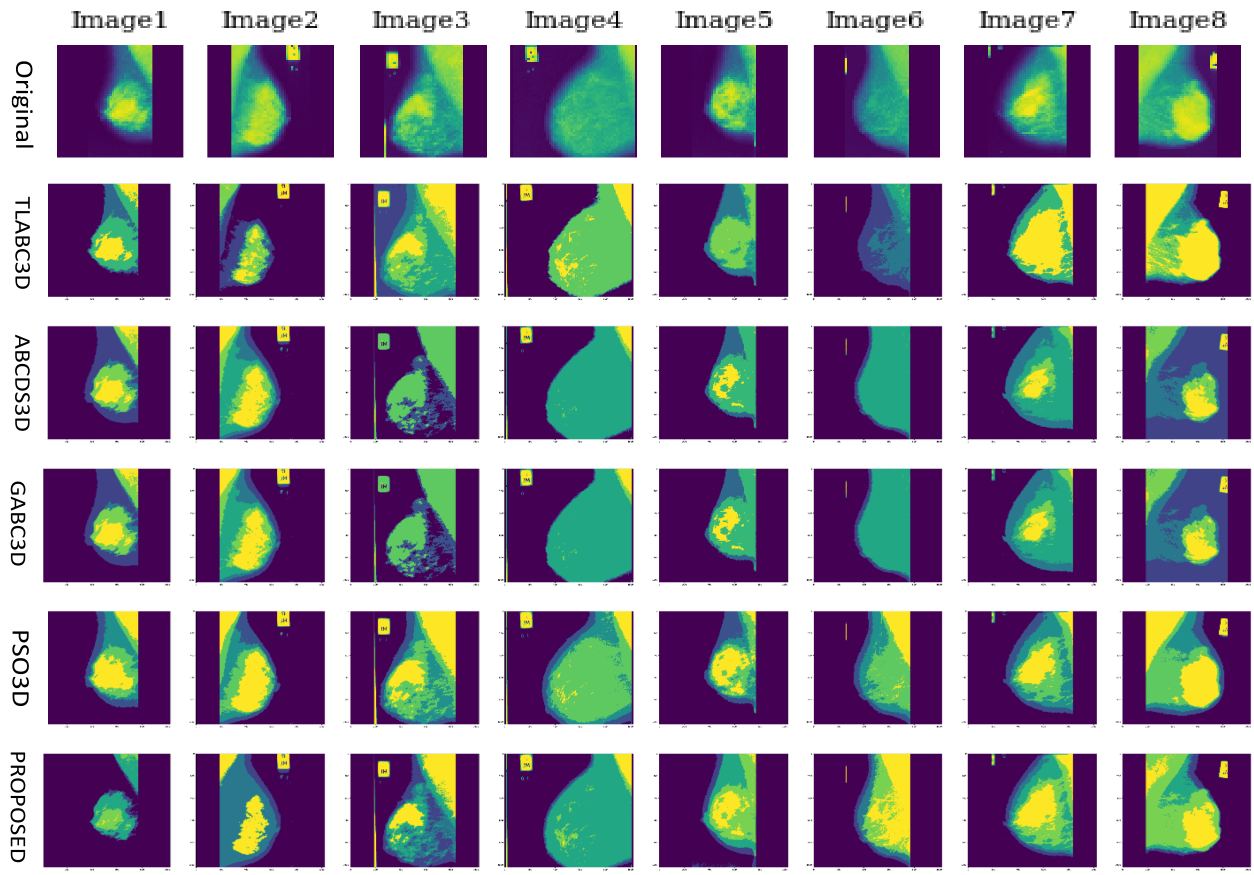

Figure. 5 Original and segmented mammogram images

2nd, 3rd, 4th, and 5th rows represent the resulted images after applying the TLABC, ABCDS, GABC, PSO and improved ABC respectively with 3D Otsu's as objective function.

The suggested technique is compared with the author's earlier work [21], in which the classic multi-otsu fitness function is utilised to optimise mammography segmentation using the ABC algorithm. The suggested technique employs a 3D histogram and requires more time (249 seconds), whereas the earlier work just requires a 1D histogram and less time (183 seconds). However, The PSNR (84%) and SSIM (31.14) values of the proposed method, significantly outperform those of the previous method [21] (PSNR is 76% and SSIM is 29.43).

Table 3. CPU Time comparison

	TLABC **[17]**	ABCDS **[18]**	GABC **[15]**	IPSO **[13]**	**ABC3D**
2-Thresholds					
Img1	487.5	425	440.6	393.8	440.6
Img2	503.1	440.6	471.9	440.6	425
Img3	487.5	440.6	503.1	471.9	425
Img4	534.4	456.3	753.1	440.6	409.4
Img5	862.5	425	503.1	425	425
Img6	925	550	440.6	425	409.4
Img7	878.1	596.9	612.5	440.6	440.6
Img8	534.4	456.3	471.9	440.6	425
3-Thresholds					
Img1	271.9	287.5	271.9	240.6	240.6
Img2	271.9	256.3	256.3	256.3	227.5
Img3	240.6	256.3	271.9	256.3	256.3
Img4	318.8	287.5	287.5	271.9	256.3
Img5	287.5	303.1	287.5	256.3	256.3
Img6	303.1	303.1	271.9	240.6	256.3
Img7	256.3	271.9	240.6	271.9	220.6
Img8	365.6	256.3	303.1	271.9	271.9
5-Thresholds					
Img1	75	76.56	75	81.25	73.44
Img2	75	76.56	75	75	78.13
Img3	81.25	87.5	76.56	73.44	73.44
Img4	78.13	76.56	76.56	76.56	78.13
Img5	78.13	75	76.56	75	73.44
Img6	75	75	75	75	73.44
Img7	76.56	75	78.13	76.56	75
Img8	76.56	76.56	81.25	76.56	75
AVG	**339.3**	**276.3**	**292**	**256**	**249**

5. Conclusion

This study proposed an improved ABC with 3D-Otsu's multi thresholding approach to identify suspicious areas on mammograms. the method, to handle the exploration-exploitation dilemma in the course of searching solution space, the epsilon greedy technique is adopted in SB phase of ABC algorithm. Moreover, Medical mammograms are segmented with 3D-for Otsu's the first time in this study since it is employed as an objective function in Improved ABC and has attained satisfactory status. The Improved ABC-3D method is employed to find the better threshold set for the eight mammograms that were taken from the MIAS database. Different threshold levels are also used to examine how well the suggested method performs. In addition, parameters like SSIM, PSNR and execution time are used to assess the standard of the ABC3D in order to confirm its competence and efficacy. The suggested algorithm took less CPU time of 249seconds whereas TLABC, ABCDS, GABC and IPSO took 339.3, 276.3, 292 and 256 seconds respectively. Moreover, ABC3D got best PSNR, SSIM values 84%, 31.14% respectively. As a result, ABC3D outperforms the majority of the conventional and cutting-edge segmentation techniques, according to the quantitative and graphical examination. Thus, in several medical image processing applications, the suggested approach may be widely employed. Future work may be done to decrease the of 3D Otsu's time complexity with similar NIOAs, and Other medical imaging datasets can be employed with the proposed methodology.

Conflicts of interest

We confirm that there is no conflict of interest in this work.

Author contributions

Conceptualization, Validation, Methodology, Writing—review and editing, M. A. Kumar and Y. Ramadevi; investigation, Writing—original draft preparation and visualization: M. A. Kumar; Formal analysis, resources, data curation and Supervision: Y. Ramdevi;

References

[1] B. O. Anderson, A. M. Ilbawi, E. Fidarova, E. Weiderpass, L. Stevens, M. A. Wahab, and B. Mikkelsen, "The Global Breast Cancer Initiative: a strategic collaboration to strengthen health care for non-communicable diseases", *The Lancet Oncology*, Vol. 22, No. 5, pp. 578-581, 2021.

[2] A. N. Giaquinto, H. Sung, K. D Miller, J. L. Kramer, L. A. Newman, A. Minihan, and R. L. Siegel. "Breast cancer statistics", *CA: A Cancer Journal for Clinicians*, Vol. 72, No. 6, pp. 524-541, 2022.

[3] S. Winters, C. Martin, D. Murphy, and N. K. Shokar, ''Breast cancer epidemiology, prevention, and screening'', *Progress in Molecular Biology and Translational Science*, Vol. 151, pp. 1–32, 2017.

[4] H. Su, D. Zhao, F. Yu, A. A. Heidari, Y. Zhang, H. Chen, C. Li, J. Pan, and S. Quan, "Horizontal and vertical search artificial bee colony for image segmentation of COVID-19 X-ray images", *Computers in Biology and Medicine*, Vol. 142, p.105181, 2022.

[5] N. Otsu, "A threshold selection method from gray-level histograms", *IEEE Transactions on Systems, Man, and Cybernetics*, Vol. SMC-9, No. 1, pp. 62–66, 1979.

[6] L. Jianzhuang, L. Wenqing, and T. Yupeng,

"Automatic thresholding of gray-level pictures using two-dimension Otsu method", In: *Proc. of International Conf. on Circuits and Systems*, pp. 325–327, 1991.

[7] X. J. Jing, J. F. Li, and Y. L. Liu, "Image segmentation based on 3-D maximum between-cluster variance", *Acta Electronica Sinica*, Vol. 31, No. 9, pp. 1281–1285, 2003

[8] A. K. Bhandari, A Ghosh, and I. V. Kumar, "A local contrast fusion based 3D Otsu algorithm for multilevel image segmentation", *IEEE/CAA Journal of Automatica Sinica*, Vol. 7, No. 1, pp. 200-213, 2022.

[9] J. Kennedy and R. Eberhart, "Particle swarm optimization", In: *Proc. of IEEE International Conf. of Neural Networks*, pp. 1942–1948, 1995.

[10] D. Karaboga and B. Basturk, "A powerful and efficient algorithm for numerical function optimization: Artificial bee colony (ABC) algorithm", *Journal of Global Optimization*, Vol. 39, No. 3, pp. 459–471, 2007.

[11] B. Wu, J. Zhou, X. Ji, Y. Yin, and X. Shen, "An ameliorated teaching-learning based optimization algorithm based study of image segmentation for multilevel thresholding using Kapur's entropy and Otsu's between class variance", *Information Sciences*, Vol. 533, pp. 72–107, 2020.

[12] D. Zhao, L. Liu, F. Yu, A. A. Heidari, M. Wang, G. Liang, K. Muhammad, and H. Chen, "Chaotic random spare ant colony optimization for multi-threshold image segmentation of 2D Kapur entropy", *Knowledge-Based Systems*, Vol. 216, p. 106510, 2020.

[13] Y Zhao, X. Yu, H. Wu, Y. Zhou, X. Sun, S. Yu, and H. Liu, "A Fast 2-D Otsu lung tissue image segmentation algorithm based on improved PSO", *Microprocessors and Microsystems*, Vol. 80, p. 103527, 2021.

[14] D. H. Wolper and W. G. Macready, "No free lunch theorems for optimization", *IEEE Transactions on Evolutionary Computation*, Vol. 1, No. 1, pp. 67–82, 1997.

[15] Zhu, Guopu, and S. Kwong, "Gbest-guided artificial bee colony algorithm for numerical function optimization", *Applied Mathematics and Computation*, Vol. 217, No. 7, pp. 3166-3173, 2010.

[16] C. Zhao, H. Zhao, G. Wang, and H. Chen, "Improvement SVM classification performance of hyperspectral image using chaotic sequences in ABC", *IEEE Access*, Vol. 8, pp. 73947-73956, 2020.

[17] X. Chen and B. Xu, "Teaching-learning-based artificial bee colony", *International Conference on Swarm Intelligence. Springer, Cham*, pp. 168-178, 2018.

[18] R. A. A. Saleh and R. Akay, "Artificial bee colony algorithm with directed scout", *Soft Computing*, Vol. 25, No. 21, pp. 13567-13593, 2021.

[19] A. A. Ewees, M. A. Elaziz, M. A. A. A. Qaness, H. A. Khalil, and S. Kim, "Improved artificial bee colony using sine-cosine algorithm for multi-level thresholding image segmentation", *IEEE Access*, Vol. 8, pp. 26304–26315, 2020.

[20] Q. Zhu, L. Jing, and R. Bi, "Exploration and improvement of Ostu threshold segmentation algorithm", In: *Proc. of 8th World Congress on Intelligent Control and Automation. IEEE, Jinan, China*, pp. 6183-6188, 2010.

[21] M. A. Kumar and Y. Ramadevi, "Multi-Otsu's image segmentation for Mammograms using Artificial Bee Colony (ABC) Algorithm", *Annals of the Romanian Society for Cell Biology*, Vol. 25, No. 4, pp. 12353-12362, 2021.

[22] Y. Feng, H. Zhao, X. Li, X. Zhang, and H. Li, "A multi-scale 3D Otsu thresholding algorithm for medical image segmentation", *Digital Signal Processing*, Vol. 60, pp. 186-199. 2017.

[23] R. S. Sutton and A. G. Barto, *Reinforcement Learning: An Introduction*. MIT press, 2018.

[24] S. A. Akanmu, R. Garg, and A. R. Gilal, "Towards an improved strategy for solving multi-armed bandit problem", *International Journal of Innovative Technology and Exploring Engineering*, Vol. 8, No. 12, pp. 5060-5064, 2019.

[25] Z. Deng and G. Zhang, "An Improved Forest Fire Monitoring Algorithm With 3D Otsu", *IEEE Access*, Vol. 9, pp. 118367-118378, 2021.

[26] J. P. Suckling, "The mammographic image analysis society digital mammogram database", *in Exerpta Medica. International Congress Series*, Vol. 1069, pp. 375-386, 1994.

[27] A. K. Garside and I Amallynda, "A Crossbreed Discrete Artificial Bee Colony for Permutation Flow Shop Scheduling Problem to Minimize Total Earliness and Tardiness", *International Journal of Intelligent Engineering & Systems*, Vol. 15, No. 1, pp. 441-451, 2021, doi: 10.22266/ijies2022.0228.40.

[28] B. S. Shihab, H. N. Abdullah, and L. A. Hassnawi, "Improved Artificial Bee Colony Algorithm-based Path Planning of Unmanned Aerial Vehicle Using Late Acceptance Hill Climbing", *International Journal of Intelligent Engineering and Systems*, Vol. 15, No. 6, pp. 431-442, 2022, doi:

10.22266/ijies2022.1231.39.

[29] M. A. Kaabi and L. A. Bahrani, "Modified artificial bee colony optimization technique with different objective function of constraints optimal power flow", *International Journal of Intelligent Engineering and Systems*, Vol. 13, No. 4, pp. 378-388, 2020, doi: 10.22266/ijies2022.0630.25.